WCTE 2014 Quebec City Canada August 10-14
World Conference on Timber Engineering

SEISMIC PROTECTION OF TIMBER PLATFORM FRAME BUILDING STRUCTURES WITH HYSTERETIC ENERGY DISSIPATORS. FEASIBILITY STUDY

Edgar Segués[1], Francisco López Almansa[2], Inmaculada R. Cantalapiedra[3]

ABSTRACT: This paper describes a feasibility study of new hysteretic energy dissipators for seismic protection of timber platform frame buildings, either for retrofit or for new construction. The system consists in connecting the timber frame to a steel framed structure that includes the new energy dissipators devices, designed to absorb most of the seismic input energy thus protecting the timber frame and the other steel members; alternatively, the system might contain other dissipative devices. The steel structure comprises horizontal beam-like elements, vertical column like elements and chevron-like bracing members; the beam-like elements are steel belts embracing each slab of the building and the bracing members hold the energy dissipators. The steel structure is self-supporting, i.e. the timber frame is not affected by horizontal actions and can be designed without accounting for any seismic provision; in turn, the steel members do not participate in the main carrying-loads system. The timber-steel contact is even, smoothed and spread; it guarantees that the yielding of the dissipators is prior to any timber failure. This research belongs to a wider project aiming to promote the structural and constructional use of timber in seismic regions; this research includes experiments and advanced numerical simulation aiming to derive accurate design criteria. Comparison with unprotected buildings and other earthquake-resistant solutions is in progress.

KEYWORDS: Timber platform frame building structures, energy dissipators, earthquake-resistant design

1 INTRODUCTION

Timber construction offers relevant environmental benefits, if wood is collected from local and sustainably exploited forests, since promotes the plantation of trees and itself stores carbon during its lifetime, thus reducing the greenhouse effect. On the contrary, the steel, concrete and masonry competing materials have high harmful environmental impacts: energy consumption, landscape destruction and air emissions. Furthermore, wooden construction presents other relevant advantages: high reusability and recyclability, moderate cost, high resistance / weight ratio, simpler foundations because of the timber lightweight, construction rapidity, insulating qualities, and nice-looking aspect. Conversely, timber has some major drawbacks for structural and constructional use: limited strength, heterogeneity and anisotropy, hygroscopicity, shrinkage, swelling, controversial fire resistance, degradability, maintenance requirements, difficulty of connections and contentious seismic resistance. This research aims to contribute to overwhelm the last two limitations by proposing additional energy dissipators devices to protect the wooden members from damage generated by seismic inputs. As is mentioned later, timber platform frame buildings are much spread and gather most of the seismic vulnerability; for these reasons, this work focuses on them.

Timber platform frame constructions with thin-paneled walls are essentially an assembly of vertical and horizontal wooden framed panels [1]. The horizontal floor and roof panels are constituted by a top wood-based sheathing board (plywood or oriented strand board OSB) supported by side and inner timber joists. The vertical panels consist of two wood-based sheathing boards also (plywood or oriented strand board OSB) framed with timber studs; the top and bottom sides of each panel are reinforced with binders (also known as rails or plates). The walls have load-bearing capacity and can be either external (cladding) or internal (partitioning). Belonging this construction technology to the platform timber frame family, the vertical panels are one-story high; can be either whole (unpierced) or with door or window openings. The sheathing boards are nailed to the framing elements i.e. joists in the horizontal panels and studs and binders in the vertical panels. The connection between the floor and wall

[1] E. Segués, Technical University of Catalonia, Barcelona. Email: edgar.segues@upc.edu
[2] F.López Almansa, Technical University of Catalonia, Barcelona
[3] I.R. Cantalapiedra, Technical University of Catalonia, Barcelona

panels is commonly established by nailing the binders to the joists. This construction type is usually considered only for buildings not exceeding six floors.

1.1 SEISMIC BEHAVIOR OF TIMBER PLATFORM FRAME STRUCTURES

Wooden constructions are, potentially, highly resistant to earthquakes due to their lightweight, to the high damping of wood, to the increased resistance of timber to rapidly varying forces, and to the high structural redundancy, mostly in the platform frame system. However, these qualities do not suffice because, under severe seismic excitations, the constructions need to be ductile; i.e. capable to absorb the input energy by means of inelastic deformations but without collapse. Contrary to a certain common belief, timber is a rather brittle material and cannot provide enough ductility to the construction; this lack impairs the seismic qualities of timber constructions, together with the important unpredictability of the damping characteristics of timber. The traditional solution to this problem consists in using mechanical connections with enough ductility but, if they are damaged after severe ground motions, such damage is mainly focused in timber, thus preventing any possibility of repair. Current research has focused in designing and testing connections with higher energy dissipation capacity [2][7], but in such connections the damage initiates in timber instead of concentrating only in the metal elements. In other words, mechanical connections are capable of absorbing part of the energy introduced by the seismic input but such energy is absorbed through irreparable damage in the timber members; moreover, in most of the cases, the energy absorption capacity is only limited. Conversely, next section 2 describes a more clever approach resting on energy dissipators.

As is described above, in the context of the seismic functioning of timber constructions the timber platform frame offers high structural redundancy and is an extreme lightweight construction. However, it suffers of a limited horizontal resistance. The lateral strength is mainly provided by the shear capacity of the vertical sheathing boards and by the nailed connections between the studs and the boards [8]. Moreover, in buildings with high plan aspect ratio, the limited strength of the slabs can hinder the diaphragm effect. Given that the lateral strength is low, it can be globally said that timber platform frame buildings are vulnerable to severe earthquakes. This vulnerability is increased when the ground floor configuration requires of diaphanous spaces.

Given the aforementioned limitations, important attention has been paid to the earthquake-resistant design of timber platform frame buildings; the NEESWood research project [9]-[13] perhaps being the clearest demonstration. That project consisted in designing, assembling and testing on shaking tables two buildings with two and six stories, respectively.

The measured fundamental periods in either horizontal direction of both buildings (0.23-0.33s in two story building and 0.41-0.42s in six story building) can be considered grossly representative of short and mid-height edifices. Hence, the timber platform frame buildings lie in the short or mid period ranges of the design energy spectra [14][17]; such ranges correspond usually to growing and to constant branches of the design spectra, respectively. Therefore, even if the supplemental dampers increase the stiffness of the building, the subsequent shortening of the fundamental period is unlike to lead to any rise of the input energy.

For timber platform frame buildings the basic earthquake-resistant design strategy [18] consists in setting enough length of lateral resisting walls and of providing them with adequate shear resistance. This objective is accomplished through the proper design of the nailed connections and using plywood sheathing board rather than OSB. Another approach rests on incorporating bracing members to the wall panels [19]. To prevent the uplift, vertical steel ties have been suggested [11]; such hold-down mechanisms are intended to limit the uplift and rocking of the stacked shear walls.

2 PROPOSED SEISMIC PROTECTION SYSTEM

Energy dissipators [20]-[21] are elements external to the main structural system, in the sense that they do not participate in the gravity-loads-carrying system. They are connected to the structure as experiencing important deformations under interstory drift motions. Through these deformations, the dissipators absorb energy, thus protecting the rest of the construction; said in a clearer way, they can be considered as “structural fuses” (i.e. the “weakest links”) of the structural chain. Furthermore, these elements can be easily replaced after having being damaged by strong earthquakes.

The hitherto proposed devices can be classified with respect to their dissipation mechanisms into: hysteretic (yielding of metals), friction, viscoelastic materials, viscous fluids, super-elasticity (shape memory alloys), among others. The hysteretic devices can provide excellent performance yet being significantly cheaper and simpler than the other dissipators are.

In most of the cases, the energy dissipators for seismic protection of building structures are connected to the main frame through additional bracing systems. Therefore, the seismic efficiency of the dissipators must be judged by comparing three major design options: bare frame (frame without any bracing), protected frame (frame with dissipative devices) and braced frame (frame with rigid connections without energy dissipators). The superiority of the second option compared to the two other is far from obvious; the paper [22][22] shows that, globally speaking, this pre-eminence can be true for mid-height or tall

buildings but in short buildings frequently a convenient option might be installing rigid bracing systems. This conclusion relies on extensive nonlinear dynamic analysis.

A number of dissipative devices have been considered for the seismic protection of timber platform frame buildings; the reference [23]-[31] presents a wide literature review. These studies clearly stated the efficiency of different types of energy dissipators for reducing the seismic response of timber platform frame buildings. However, these researches do not investigate the capacity of the dissipative system to absorb the damaging part of the input energy.

The offered technology has been designed to fulfill the requirements stated in section 2 along with compatibility with the current timber construction practice; emphasis has been placed on economy, simplicity, ease of production and installing, robustness, and low maintenance requirements. Consequently, only timber and steel elements are used, without chemical connections; as well, the derived solutions offer a high degree of prefabricability.

The proposed earthquake-resistant solution results from the combination of two parallel-connected structural systems: a traditional timber platform frame and an additional peripheral steel bracing system including hysteretic energy dissipators. The design of both systems and of their connection allows that the timber frame carries the gravity loads and the steel members take the forces generated by horizontal actions, e.g. wind and earthquakes. In other words, the vertical and horizontal actions are separately withstood by the timber and steel structural systems, respectively; i.e. the timber/steel structures are designed without accounting for any horizontal/vertical action, respectively.

The proposed solution is primarily meant for timber platform frame buildings with symmetric rectangular plan configuration, i.e. without relevant re-entrant corners or edge recesses, and with uniformity along the height, i.e. without significant setbacks. The steel protective system is formed of four vertical truss-like planar structures connected to each of the building façades by steel belts, as shown by *Figure 1*. This layout is intended to provide plan symmetry and torsion strength; special attention has been paid to this last issue, giving the aforementioned torsion effects detected in the NEESWood research project [11].

Figure 1Figure 1.b displays a 3-story timber building incorporating a steel protective structure including energy dissipators at each story; such devices are flexible steel plates which are intended to yield (and thus, to dissipate energy) under interstory drift motions. The truss-like steel structure comprises: (i) column-like vertical members, which are continuous down to foundation, (ii) horizontal plate members embracing the whole building at each story level thus constituting a kind of confining steel belt and (iii) single-story trusses.

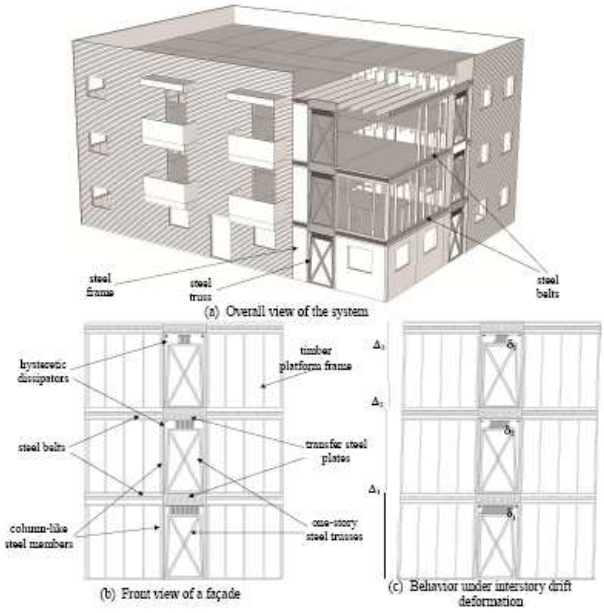

Figure 1 *Proposed steel seismic protection system*

The connections among these members will be rigid. The column-like vertical members have two purposes: to transmit to the foundation the vertical forces generated by the horizontal shear forces in the flexible steel plates, and to provide residual lateral stiffness to the building after the yielding of the flexible plates. The plated steel belt is continuously joined to the adjacent timber header joist by nailing or other equivalent mechanical connectors. The segments of the belt that are right above the dissipative devices are locally reinforced to guarantee the transmission of forces between the steel members of adjoining stories; such stiffened segments are termed as “transfer steel plates”, see *Figure 1*.b. In each floor, the dissipators are rigidly connected by their lower end to the aforementioned single-story rigid truss and by their upper end to the top transfer steel plate. Under seismic excitation, the massive floor slabs draw the steel belts; the subsequent interstory drift motion generates strains in the devices, as shown by *Figure 2*.b The steel belts will be prestressed to avoid separation from the timber beams due to wood shrinkage or local wood compression; in this way, when the timber mass is pushing, the steel-timber stresses transfer will be generated mainly by compression of the front timber beams and by friction along the side timber beams. Furthermore, since the steel belts produce a certain confinement of the slabs, an additional benefit of this solution is an improved diaphragm behavior.

As discussed in section 2 the dissipators must constitute the “weakest link” in the lateral resisting system, namely, the yielding of the dissipative devices should be prior to any other failure. Since steel is a lot more resistant than timber, a highly distributed, even and smoothed contact between both materials is pursued. As discussed in the

previous paragraph, this objective is accomplished mainly through the steel belts.

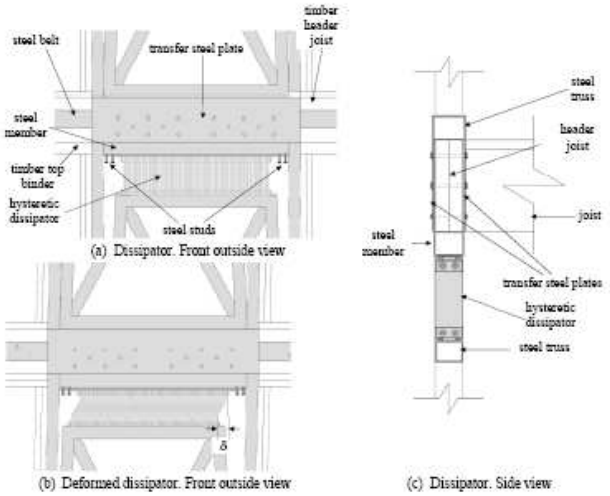

Figure 2 *Energy dissipators installed in the steel frame*

Figure 2 displays details of the connections between the dissipators, the steel structure and the timber frame. The connection between the dissipative devices and the lower truss is completely rigid. Conversely, the connection with the upper steel members allows for vertical sliding, yet guaranteeing the compatibility between horizontal displacements; the purpose of this capability is to accommodate the vertical down displacement of the upper part of the dissipators caused by the big strains of the flexible steel plates, see *Figure 2*.b. *Figure 2* points out that such vertical sliding condition is attained through steel studs with prestressed coil springs; the studs are fixed to the upper steel member and go across the top plate of the dissipators through pre-milled holes. The prestressed springs provide re-levelling capacity. The gap between the studs and the pre-milled holes in the upper steel member will be minimized to reduce the influence of pinching in the hysteresis loop of the dissipators.

Each energy dissipator device contains two parallel steel rigid plates and a series array of a number of smaller parallel flexible (thin) steel plates. The rigid plates are termed “anchorage plates”, since they are connected to the top transfer steel plate and to the bottom steel truss, respectively (*Figure 2*). Each flexible plate is clamped at both ends to a holding set. This configuration causes that the interstory drift motion generates plastic bending deformation of the flexible plates, thus dissipating energy. The holding sets are composed “steel separators” to guarantee the separation between adjacent flexible plates and two “end rigid bodies”. The separators are rectangular steel plates and the end bodies are L-shaped with two stiffening gusset plates. The separators, the flexible plates and the end bodies are perforated as to be threaded and prestressed by high strength steel bolts; this prestressing effect guarantees the clamping of the flexible plates. The devices are able to hold to any number of flexible plates with different sizes. Both constant-width and X-shaped plates [32] might be considered.

Re-centering capabilities might be provided, if deemed necessary. Additionally, it should be pointed out that the proposed steel system can add some strength to strong winds, such as hurricanes and tornadoes.

3 DISSIPATIVE BEHAVIOR OF THE PROPOSED DEVICES

This section describes the dissipative behavior of the flexible steel plates; see *Figure 3*.a represents the deformation of a given flexible steel plate and *Figure 3*.b depicts the ensuing force-displacement law; the plots in *Figure 3*.b have been derived assuming an elastic-perfectly-plastic behavior for the steel. In *Figure 3*.a, l is the clear length and t and b are the thickness and the width of the plate, respectively; F and $F\,l\,/\,2$ are the reaction forces and δ is the transverse displacement of the plate. *Figure 3*.b shows that the force-displacement law has an initial linear elastic branch followed by a curved plastic branch. F_{el} and δ_{el} are the force and the displacement that correspond to the onset of yielding in the extreme sections; after that, yielding is progressing and the curve is accordingly becoming less steep. Once the plastification of the extreme sections is completed, plastic hinges are formed and the plate loses utterly its stiffness; therefore, the plastic branch approaches asymptotically to the yielding force F_y. For modelling purposes, a bilinear diagram whose initial branch has the same slope than the elastic one and the second branch is horizontal represents the actual law. *Figure 3*.b shows that the corner displacement δ_y can be read as the yielding displacement of the bilinear model.

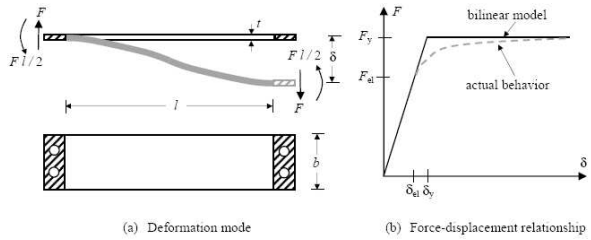

Figure 3 *Dissipative Behavior of a flexible steel plate*

By performing simple linear elastic analyses neglecting the contribution of the shear force to the deflection, the following closed-form relations among the involved elastic quantities are obtained:

$$\delta_{el} = \frac{f_y\, l^2}{3\, E\, t} \qquad F_{el} = \frac{f_y\, b\, t^2}{3\, l} \qquad k = E\, b \left(\frac{t}{l}\right)^3 \quad (1)$$

In equation (1), E and f_y are the steel modulus of elasticity and yielding point, respectively, and k is the stiffness of the force-displacement elastic branch, given by $F = k\,\delta$. Given

that the plastic moment of a rectangular section is equal to 1.5 times the elastic one, it follows immediately that

$$\delta_y = 1.5\,\delta_{el} = \frac{f_y\, l^2}{2\,E\,t} \qquad F_y = 1.5\,F_{el} = \frac{f_y\, b\, t^2}{2\,l} \tag{2}$$

In the derivation of equations (1) and (2), the plastic interaction between the shear force and the bending moment has been neglected. This assumption holds as long as *l* is significantly bigger than *t*.

Under reverse cycling motion, the bilinear behavior depicted in *Figure 3*.b turns into the hysteresis loop displayed in *Figure 4* δ_{max} accounts for the maximum transverse displacement. The smoothed branches of the unloading branches are typical of hysteretic devices [33].

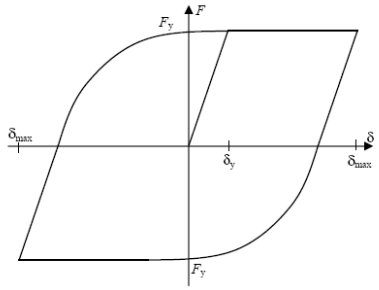

Figure 4 *Hysteresis loop of a flexible steel plate*

The energy dissipated in one cycle is equal to the area encompassed by the loop displayed in *Figure 4* for a given seismic input the absorbed energy E_d depends on many parameters, such as yielding force, maximum displacement, duration, impulsivity, and frequency content, among others. However, in normal conditions it might be grossly accepted that such energy is only related to the yielding force and the maximum displacement; such conclusion relies on the assumption that the displacement ductility ($\mu = \delta_{max} / \delta_y$) and the cumulative ductility (in a single device, $\eta = E_d / F_y\,\delta_y$) are related by the approximate relation $\eta = 4\,(\mu - 1)$ [34]:

$$E_d = \eta\, F_y \delta_y = 4\,(\mu - 1)\, F_y \delta_y = 4\left(\frac{\delta_{max}}{\delta_y} - 1\right) F_y \delta_y = 4 F_y \left(\delta_{max} - \delta_y\right) \approx 4 F_y \delta_{max} \tag{3}$$

Equation (3) holds if μ is sufficiently high, so that $\mu - 1$ can be approached by μ.

4 SEISMIC DESIGN BASED ON INPUT ENERGY SPECTRA

In conventional earthquake-resistant design of buildings and other constructions, the dynamic effect of the input ground motion is represented by static equivalent forces, which are obtained from acceleration response spectra defined as the ratio between the peak ground acceleration and the maximum absolute acceleration in the top of the construction. This approach entails several drawbacks: (i) these equivalent forces are strongly coupled to the elastic and hysteretic characteristics of the structure, thus making seismic design cumbersome, (ii) after the onset of yielding, the correlation between the design forces and the structural damage is poor, and (iii) the damage caused by the cumulative inelastic excursions [35] is not accounted for. More recently, displacement-based design procedures have been proposed [36]; in these strategies, the dynamic effect of the input is represented by imposed displacements, in turn obtained from displacement response spectra relating the design ground acceleration to the maximum relative displacement in the top of the building. This formulation partially uncouples the input effect –in terms of displacement– from the characteristics of the structure and allows for a satisfactory correlation between the imposed displacement and the component of the structural damage that is related to the maximum displacement. Conversely, in this formulation, the component of damage that is related to the cumulative plastic strain energy cannot be appropriately considered. A more rational seismic design approach, which also overcomes this difficulty, consists in expressing the dynamic input effect through energy response spectra via the Housner-Akiyama energy formulation [20] and [34]. Interpreting the effect of earthquakes in terms of energy is gaining extensive attention [37]-[40]. This approach features three major advantages: (i) the input effect in terms of energy and the structural resistance in terms of energy dissipation capacity are basically uncoupled, (ii) except in the short period range, the input energy, E_I, introduced by a given ground motion in a structure is a stable quantity, governed primarily by the natural period *T* and the mass *m*, and scarcely affected by other structural properties such as resistance, damping and hysteretic behavior, and (iii) the consideration of the cumulative damage can be directly addressed. In the energy-based methods, the design criterion resides in the comparison between the seismic resistance of the structure in terms of energy absorption capacity and the effect of the ground motion in terms of input energy. It is then necessary to establish the E_I input energy spectrum corresponding to the expected earthquake, i.e. design input energy spectrum. The structure is able to absorb, through damping, a part E_ζ of the input energy and the remaining part is dissipated by additional structural damage; this damaging part of the input energy is commonly termed as hysteretic energy E_H [41]. Once the kinetic and elastic energies have vanished, the energy balance equation can be written as

$$E_\zeta + E_H = E_I \tag{4}$$

If the dynamic behavior of the building is described by lumped masses models, then

$$E_\zeta = \int \dot{\mathbf{x}}^T \mathbf{C}\, \dot{\mathbf{x}}\, dt \qquad E_I = -\int \dot{\mathbf{x}}^T \mathbf{M}\mathbf{r}\, \ddot{x}_g\, dt \tag{5}$$

C is the viscous damping matrix, **M** is the mass matrix, $\dot{\mathbf{x}}$ is the relative velocity vector, **r** is the influence vector and

$\ddot{x}_g$ is the input ground acceleration; for 2D models of plan symmetry buildings $\mathbf{r} = (1,\ldots,1)^T$. The energy-based design is particularly well suited for constructions incorporating energy dissipators: they are designed to absorb the hysteretic energy. In other words, the energy dissipated jointly by all the devices E_D should be bigger or equal than E_H:

$$E_D \geq E_H \tag{6}$$

Commonly, E_I and E_H are normalized with respect to the mass m of the building and expressed in terms of equivalent velocities V_E and V_D:

$$V_E = \sqrt{2E_I / m} \quad V_D = \sqrt{2E_H / m} \tag{7}$$

For practical energy-based earthquake-resistant design, V_E is obtained from available design energy spectra and V_D is estimated from V_E through empirical expressions of the ratio V_D / V_E: V_D = V_E (V_D / V_E). Among other researchers, [14] proposed design energy input spectra for moderate seismicity regions and [15] and [16]-[17], proposed design energy input spectra for moderate-to-high seismicity regions based on Colombian and on Turkish registers, respectively. These V_E input energy spectra depend on the soil characteristics (stiff / soft), the seismic design acceleration, the magnitude of the expected earthquakes ($M_s \leq 5.5$ and $M_s > 5.5$) and the type of seismic input (impulsive / vibratory registers); conversely, they do not depend neither on the mass nor on the damping parameters. Moreover, except in the short period range, the V_E spectra are also independent of the hysteretic behavior of the structure. A number of researchers [15-[17] [34], [35] [37]; have derived empirical expressions of the ratio V_D / V_E; such expressions depend on the soil type, the structural damping ζ, the fundamental period of the structure T_F, and the displacement ductility μ.

5 DESIGN OF THE PROPOSED SYSTEM

This section presents simplified, yet sound and reliable, design criteria of the proposed protective system. In the framework of the Performance-Based Design (PBD), the Immediate Occupancy (IO), Life Safety (LS) and Collapse Prevention (CP) performance levels are accounted for [43]. For buildings of normal importance, such levels correspond to 72, 475 and 970 years return period, respectively [44].

The design consists in selecting the geometrical and mechanical parameters of the flexible steel plates (b, l, t and f_y) and the number of plates per level and per direction (n_{pi}) trying to fulfill the requirements for the 3 considered performance levels.

The design value of the stiffness k and the yielding force F_y of a given plate can be stated separately after equations (1) and (2) in terms of the geometrical parameters b, t and l. For the sake of simplicity, all the flexible steel plates can be designed alike since the possibility of choosing separately the number of plates for each story allows sufficiently for a tailored design. For any series array of flexible steel plates *Figure 1* the joint yielding force and stiffness are equal to those of each plate times the number of plates:

$$V_{yi} = F_y n_{pi} \qquad K_i = k n_{pi} \tag{8}$$

In equation (8), V_{yi}, K_i and n_{pi} are the yielding shear force, the shear stiffness and the number of flexible steel plates of the i-th story in a given direction (two opposite façades), respectively. Conversely to the uniform distribution described by equation (8), for the whole building in a given direction, the total dissipated energy depends also on the distribution among the different stories and on the accidental eccentricities. The variation of the design yielding forces along the building height can be based either on the complex approaches in [34] and [45] or on the simpler method in [22]. The formulations of [34] and [45] are based on a number of nonlinear time-history analyses and aim to obtain a rather uniform distribution of the cumulative inelastic deformation ratio η in each level along the building height. In both studies, the yielding force is normalized with respect to the weight above that floor:

$$\alpha_i = \frac{V_{yi}}{\sum_{j=i}^{N} W_j} \tag{9}$$

N is the number of floors. According to Akiyama, the distribution of α_i obeys to two polynomial expressions:

$$\frac{i-1}{N} < 0.2 \quad \frac{\alpha_i}{\alpha_1} = 1 + 0.5\frac{i-1}{N} \tag{10}$$

$$\frac{i-1}{N} \geq 0.2 \quad \frac{\alpha_i}{\alpha_1} = 1 + 1.5927\frac{i-1}{N} - 11.3519\left(\frac{i-1}{N}\right)^2 + 42.5883\left(\frac{i-1}{N}\right)^3 - 59.3827\left(\frac{i-1}{N}\right)^4 + 30.1586\left(\frac{i-1}{N}\right)^5$$

In the study by Benavent-Climent, the variation of α_i obeys to an exponential equation:

$$\frac{\alpha_i}{\alpha_1} = \exp\left[\left(1 - 0.02\frac{k_1^T}{k_N^T} - 0.16\frac{T_F}{T_G}\right)\frac{i-1}{N} - \left(0.5 - 0.05\frac{k_1^T}{k_N^T} - 0.3\frac{T_F}{T_G}\right)\left(\frac{i-1}{N}\right)^2\right] \tag{11}$$

In equation (11), k_i^T is the lateral stiffness of the i-th timber floor, T_F is the fundamental period of the building in the direction under consideration and T_G is the corner period of the V_E design spectrum; T_G period separates the initial growing and the horizontal branches. Since the lateral resistance of the timber frame is neglected compared to the steel system, in the considered timber platform frame buildings it can be assumed reasonably that the vertical

distribution of the lateral timber stiffness is constant; therefore: $\frac{k_1^t}{k_N^t} = 1$.

The formulation described in [22] relies on representing the effect of the expected seismic action in terms of equivalent static forces; then, the yielding force at each story V_{yi} is selected as a given percentage of the corresponding internal shear forces in each of the arrays of flexible steel plates. Usually, the considered percentages range in between 50 and 100%.

If the vertical variation of α_i is selected according to the aforementioned researches [22], [34] and [45]; the cumulative inelastic deformation ratio η in each floor is expected to be rather uniform along the building height. The aforementioned approximate closed-form relation between η and μ ($\eta = 4(\mu - 1)$, [34]) indicates that the distribution of μ will be also rather uniform; since $\mu = \delta_{max} / \delta_y$, if δ_y is the same in all the floors, the vertical distribution of the maximum transverse displacement $\delta_{max,i}$ will be also approximately constant. Hence, according to equations (3) and (8), the energy dissipated in the whole building is:

$$E_D = \frac{1}{\gamma}\sum_{i=1}^{N} E_{di} n_{yi} = \frac{1}{\gamma}\sum_{i=1}^{N} 4 F_y \delta_{max,i} n_{yi} = \frac{1}{\gamma}\sum_{i=1}^{N} 4 V_{yi} \delta_{max,i} = \frac{4\delta_{max}}{\gamma}\sum_{i=1}^{N} V_{yi} \qquad (12)$$

In equation (12), γ is a safety factor accounting globally for the irregular distribution of $\delta_{max,i}$ among the different stories and for accidental eccentricities.

The proposed design approach consists in selecting the geometrical and mechanical parameters of each flexible steel plate (b, l, t and fy) and of the number of plates per level and per direction npi to fulfill the requirements for IO, LS and CP conditions. Given the strong interdependence among the involved quantities, the design process must be carried iteratively following a trial-and-error strategy. In future stages of research, more refined design criteria will be derived. They will be based on extensive nonlinear analyses of the building equipped with the protective steel system and undergoing seismic inputs representative of the actual seismic hazard conditions. The behavior of the timber members and the steel structure will be described with the aforementioned advanced numerical models to be developed. The steel members other than the flexible steel plates can be designed later; they should yield after the flexible plates and be significantly stiffer. This higher stiffness allows minimizing the difference between the interstory drift Δ and the transverse displacement δ.

6 APPLICATION EXAMPLE

This section describes an application of the proposed system to a six-story timber platform frame apartment building located in New Zealand [46]. The building was originally designed following the former New Zealand seismic design code [47]; an alternative earthquake-resistant approach based on the proposed technology is described here. This case has been chosen to correspond to a very demanding situation: the building is as tall as it allows the chosen structural solution, the weight of the building is comparatively high, the seismic hazard is very important and the soil is rather soft.

The considered building has a rectangular floor plan with a footprint of approximately 21 m by 31 m; the height is about 18 m. The soil is classified as type D according to the current New Zealand seismic design code [48] ("Deep or soft soil"). Since the building is uniform along its height, it fits the requirements for the proposed technology. More details of the walls diaphragms configuration are given in the reference[46].

In the seismic design, a damping factor of 5% was assumed. By numerical analysis, the fundamental period was found to be approximately T_F = 1 s. This period, combined with the use of a displacement ductility factor μ = 4 and the site subsoil properties led to a design base shear coefficient $V / W = 0.15$; V is the base shear force and W is the weight of the building. The design wind loads were considerably exceeded. According to the New Zealand regulations [47] the building was also designed for serviceability conditions under a base shear coefficient $V / W = 0.10$. The weight was W = 11 MN corresponding to the load combination $D + 0.4\,L$ [47]; D and L account for dead and live load, respectively. Noticeably, the structural analysis showed that the components of the drift deformation were typically: base rotation 28%, plywood shear < 1%, nail slip 59%, and flexural deformation 12%.

6.1 ALTERNATIVE EARTHQUAKE-RESISTANT SOLUTION

The proposed alternative solution consists in designing the timber frame for gravity loads only and in designing the steel structure to resist the horizontal actions, mainly the seismic ones. It is estimated that the important reduction of horizontal demanding forces on the timber members would lead to a relevant weight reduction, from the elimination of steel bracing members and from the use of thinner and lighter sheathing boards; this weight reduction grossly compensates the steel added weight.

Immediate Occupancy. The seismic demand in the Immediate Occupancy damage state is quantified in terms of design acceleration spectra; such spectra are obtained from the New Zealand code [48]. The base shear coefficient for the plateau of the design spectrum for IO conditions is given by

$$\frac{V}{W} = \frac{C_h(T) \times Z \times R_s \times N(T,D) \times S_p}{k_\mu} = \frac{3 \times 0.4 \times 0.4 \times 1 \times 0.7}{2} = 0.168 \qquad (13)$$

$C_h(T)$ is the plateau spectral ordinate, Z is the hazard factor, R_s is the return period factor for 75 years return period, $N(T,D)$ is the near-fault factor, S_p is the structural performance factor, and k_μ is the response reduction factor. According to [49] it has been assumed that $k_\mu = 2$.

The flexible steel plates should not yield under the base shear force corresponding to the new initial stiffness of the building, e.g. before the yielding of the flexible steel plates.

Life Safety. The design for the Life Safety damage state is based on inequality (6) where the demanding hysteretic energy E_H is determined after input energy V_E spectra corresponding to 475 years return period. The V_E spectra depend on the soil characteristics (stiff / soft), the seismic design acceleration, the magnitude of the expected earthquakes ($M_s \leq 5.5$ and $M_s > 5.5$) and the type of seismic input (impulsive / vibratory registers). Given the high local seismicity and the extreme proximity to an active fault, it can be conservatively assumed that $M_s > 5.5$ and that the expected accelerograms will be mainly impulsive. For the soft soil condition, the V_E spectrum proposed in [16][17]; from Turkish registers is shown in *Figure 5* .a. For linear analyses, the spectrum in *Figure 5*.a contains an initial linearly growing branch in the short period range (0–0.32 s), a plateau in the mid period range (0.32–1.60 s) and a descendant branch with exponent 0.8 in the long period range (1.60–4.00 s). Except in the short period range, the input energy is a highly stable quantity [34] with respect to the hysteretic and damping parameters of the structure under consideration. Therefore, for nonlinear behavior (i.e. $\mu > 1$) the only required modification is an increase of the initial growing branch slope. This slope increase will result in a reduction of the lowest corner period; for $\mu = 20$ the ratio between both slopes is 1.78 [16][17], therefore, the corner period becomes 0.32 / 1.78 = 0.18 s. Both the linear and nonlinear spectra are characteristic, i.e. correspond to the 95% percentile, and are referred to 475 years return period.

The V_D spectrum is commonly obtained by multiplying the V_E spectrum by a convenient value of the V_D / V_E ratio; such ratio depends mainly on the damping factor ζ, the displacement ductility μ and the building fundamental period T_F. References [16][17] contain linear regression studies providing average expressions $V_D / V_E = a\ T_F + b$ where coefficients a and b depend on ζ, μ and T_F. The hysteretic energy can be obtained after equivalence equation (7). This seismic demand in terms of hysteretic energy can be coarsely compared with the requirements of the [48]. The comparison relies on the loose equivalence between the hysteretic energy V_D and the pseudo-velocity spectrum [34], obtained by multiplying the pseudo-acceleration spectrum by $T / 2\ \pi$. For soil type D, in the New Zealand code, the mid period range extends from 0.6 to 3 s; comparison with *Figure 5*.a shows that such range is narrower and begins in a longer period. The pseudo-velocity spectral ordinates for 0.6 and 3 s are 112 and 133 cm/s, respectively; assuming that the V_D / V_E ratio is equal to 0.825 [16][17], the corresponding V_E velocities are 136 and 161 cm/s, respectively.

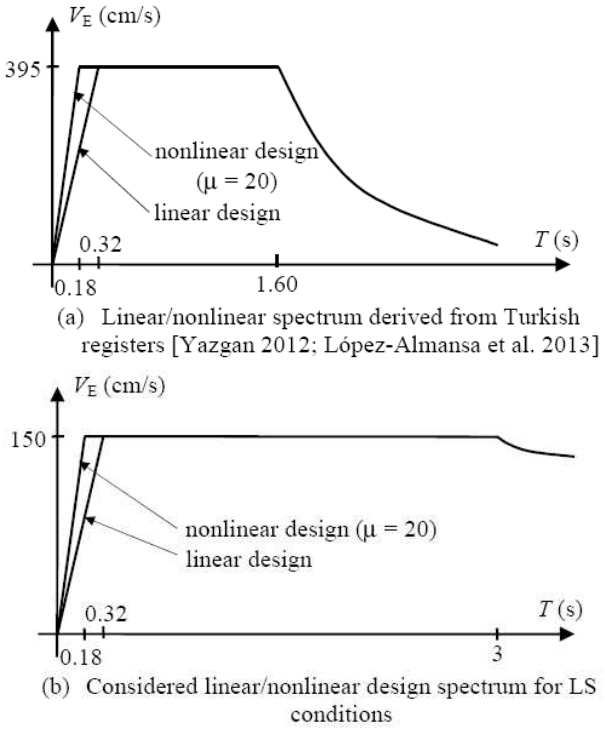

Figure 5 *Input energy design spectra*

Comparison with the spectral ordinate of the plateau in *Figure 5*.a (395 cm/s) indicates that such spectrum is significantly more demanding than the New Zealand code; it can be roughly accepted that, in the mid period range, the equivalence factor is about 2.65. *Figure 5*.b presents the considered design energy spectrum; the mid period branch is horizontal, the spectral ordinate is selected as a smoothed average of 136 and 161 cm/s, and the mid period ranges from the smallest values from *Figure 5* .a to the biggest values from the New Zealand code.

Collapse Prevention. The CP design input energy spectrum is obtained by multiplying the V_E spectrum corresponding to the LS damage state (*Figure 5*.b) by the return period factor R_u indicated in the New Zealand code [48] for 1000 years return period: $R_u = 1.3$. This consideration relies on assuming that the statistical behavior of energy spectra in terms of velocity is similar to the one of acceleration spectra. The V_D spectrum is obtained as for the LS damage state (previous subsection) by multiplying the V_E spectrum by the corresponding V_D / V_E ratio.

6.2 VERTICAL DISTRIBUTION OF THE YIELDING SHEAR FORCES OF EACH STORY

The vertical distribution of the yielding shear forces V_{yi} of the *i*-th story is selected in this subsection following the three approaches described in section 5 It is initially assumed that the fundamental period of the building after the yielding of the flexible steel plates is $T_F = 1$ s and that

the corner period corresponding to the characteristic spectrum is T_G = 0.32 s [16][17], see *Figure 5*. Given that $k_1^t = k_N^t$ (section 5), equation (11) converts into:

$$\frac{\alpha_i}{\alpha_1} = \exp\left[\left(0.38 - 0.16\frac{T_F}{T_G}\right)\frac{i-1}{6} - \left(0.45 - 0.3\frac{T_F}{T_G}\right)\left(\frac{i-1}{6}\right)^2\right] = \exp\left[0.48\frac{i-1}{6} + 0.49\left(\frac{i-1}{6}\right)^2\right] \quad (14)$$

In the formulation from [22], the internal forces in the dissipative steel elements are obtained according to the vertical distribution of the base shear force stated by the current New Zealand seismic design code [48]: $F_i = F_t + 0.92\ V\ W_i\ h_i\ /\ \Sigma_{1\le i\le N}\ W_i\ h_i$; h_i is the height above the ground and $F_t = 0.08\ V$ at the top level and zero elsewhere.

*Table 1. Vertical distribution of the yielding shear force of each story (Vyi / Vy1). Example building*displays the yielding shear force of each story V_{yi} normalized with respect to the one of the first story V_{y1}.
Table 1 shows that the three considered approaches provide similar vertical variations of the yielding force; therefore, a smoothed average shown in the last row of *Table 1* and is considered in this application example.

Table 1*. Vertical distribution of the yielding shear force of each story (V_{yi} / V_{y1}). Example building*

	Floor No.					
Approach	1	2	3	4	5	6
Akiyama 1985	1	0.903	0.787	0.691	0.545	0.362
Benavent-Climent 2011	1	0.915	0.826	0.719	0.571	0.349
Foti et al. 1998	1	0.956	0.868	0.737	0.562	0.343
This work	1	0.92	0.83	0.72	0.56	0.35

Since, as stated above the yielding of the plates should be prior to any other failure, the other steel members have to be designed as to provide higher stiffness and strength. The design is carried out iteratively as a trial-and-error process. ***Table 2*** shows two feasible choices of b, l, t, f_y and $n_{p1},\ldots,n_{p6}$. For each set of values, *Table 2* displays also the stiffness k and the yielding force F_y of an individual steel plate and the fundamental period T_F of the building prior to the yielding of the flexible steel plates. For IO, LS and CP conditions, the maximum obtained interstory drift Δ_{max} is presented; for IO, the number in parenthesis specifies the floor where the maximum drift is generated, and the base shear coefficient V / W is also displayed. Under IO, LS and CP conditions, Δ_{max} should be smaller than the threshold values indicated in sections 5 and 6, this condition being the major design criterion. For LS and CP conditions, the resulting displacement ductility μ, the corresponding V_D / V_E ratio and the demanding hysteretic energy E_H are also shown.

The calculation of the figures in ***Table 2*** is described next. After b, l, t and f_y, equations (1) and (2) provide δ_y, k and F_y. T_F is determined by a classical eigenvalue analysis neglecting the contribution of the timber members and the steel truss to the lateral stiffness; the stiffness K_i of each array of flexible steel plates is given by equation (8).

Table 2. *Feasible sets of parameters of the dissipative elements in the example building. f_y = 550 MPa. γ= 1.25. ζ = 0.05*

		bllll **(mm)**	
		150/180/12	150/150/8
$n_{p1}/n_{p2}/n_{p3}/n_{p4}/n_{p5}/n_{p6}$		60/56/50/44/34/22	110/100/92/80/62/40
k **(kN/mm)**		9.33	4.78
δ_y **(mm)**		3.54	3.68
F_y **(kN)**		33.00	17.6
T_F **(s)**		0.52	0.53
IO.	***V/W***	0.168	0.168
Δ_{IO} = 30 (mm)	Δ_{max} **(mm)**	3.45 (3)	3.67 (3)
LS. Δ_{LS} = 60 (mm)	**μ**	8.5	8.7
	V_D **/** V_E	0.842	0.842
	E_H **(kNm)**	877	877
	Δ_{max} **(mm)**	31	32
CP. Δ_{CP} = 120 (mm)	**μ**	13.5	13.6
	V_D **/** V_E	0.851	0.851
	E_H **(kNm)**	1337	1337
	Δ_{max} **(mm)**	48	50

For the IO state, the base shear coefficient V / W is obtained from the design acceleration spectrum (subsection 6.1) and the maximum drift is computed by linear static analysis. For the IO and LS states, the demanding hysteretic energy E_H is got from the corresponding V_E design input energy spectrum (subsection 6.1) by using the V_D / V_E ratio and equation (7), the maximum interstory Δ_{max} is computed from equation (12) by assuming that Δ_{max} = δ_{max} (i.e. the steel trusses are assumed to be infinitely rigid compared with the flexible steel plates, see *Figure 1*.c, and the displacement ductility is stated as the ratio between Δ_{max} and δ_y.

7 CONCLUSIONS

This work proposes a new seismic protection system for timber platform frame regular buildings, both for new constructions and retrofit. The building is embraced with an outer steel structure, designed to take the lateral forces arising from the seismic excitation. The outer steel structure includes newly designed hysteretic energy dissipators; those devices are intended to absorb most of the damaging energy induced by the earthquake, thus protecting the rest of the steel structure and, mainly, the timber elements. Noticeably, the proposed system might hold any other type of dissipative devices. To highlight the practical feasibility of the proposed technology, an application to a timber platform frame building is considered. The building is 6-story and undergoes extremely severe seismic hazard, given the local seismicity, the close proximity to an active fault, and the soft soil condition; therefore, an important amount of energy has to be dissipated. Under these harsh conditions, the members of the protective steel structure are designed

in the framework of the Performance-Based Design following an energy-based design approach; the IO, LS and CP levels are considered. The obtained reasonable size of the steel elements confirms the feasibility of the proposed system. Future research will involve testing and advanced numerical simulation of the designed devices; the main objective of the research is to derive accurate design criteria.

AKNOWLEDGEMENTS

This work has received financial support from the Spanish Government under projects CGL2011-23621 and BIA2011-26816 and from the European Union (Feder).

REFERENCES

[1] Handbook 1. (2008). Timber Structures. Leonardo da Vinci Pilot Project CZ/06/B/F/PP/168007. Educational Materials for Designing and Testing of Timber Structures - TEMTIS. European Commission.

[2] Andreolli M., Piazza M., Tomasi R., Zandonini R. (2011). Ductile moment-resistant steel-timber connections. Structures and Buildings. 164(SB2) 65-78.

[3] Awaludin A., Sasaki Y., Oikawa A., Hirai T., Hayashikawa T. (2007). Friction damping of pre-stressed timber joints. Graduate School of Agriculture, Hokkaido University, Sapporo, Japan.

[4] Leijten A.J.M., Ruxton S., Prion H., Lam F. (2006). Reversed-cyclic behaviour of a novel heavy timber tube connection. Journal of Structural Engineering 132 1314-1319.

[5] Parisia M., Piazza M. (2002). Seismic behaviour and retrofitting of joints in traditional timber roof structures. Soil Dynamics and Earthquake Engineering. 22 1183-1191.

[6] Piazza M., Polastri A., Tomasi R. (2011). Ductility of timber joints under static and cyclic loads. Structures and Buildings. 164(SB2) 79-90.

[7] Popovski M., Karacabeyli E. (2012). Seismic Behaviour of Cross-Laminated Timber Structures. 15th World Conference on Earthquake Engineering (WCEE). Paper 3565. Lisbon.

[8] Hoekstra T. (2012). Multi-storey timber frame building – Modelling the racking stiffness of timber-frame shear-walls. MSc Thesis. TU Delft.

[9] Christovasilis I.P., Filiatrault A., Wanitkorkul A. (2007). Seismic testing of a fullscale two-story wood light-frame building: NEESWood benchmark test. NEESWood Report No. NW-01, Dept. of Civil, Structural and Environmental Engineering, University at Buffalo, State University of New York, Buffalo.

[10] Shinde J.K., Symans M.D., Liu H., van de Lindt J.W. (2008). Seismic performance assessment of wood-framed structures with energy dissipation systems. Proceedings of the 2008 Structures Congress, Vancouver.

[11] Pei S., van de Lindt J.W., Pryor S.E., Shimizu H., Isoda H. (2010). Seismic Testing of a Full-Scale Mid-Rise Building: The NEESWood Capstone Test. Report NW-04. Colorado State University.

[12] Lindt J.W. van de, Pei S., Pryor S.E., Shimizu H., Isoda. (2010). H. Experimental Seismic Response of a Full-Scale Six-Story Light-Frame Wood Building. J. Struct. Eng.136 1262-1272.

[13] Filiatrault A., Christovasilis I.P., Wanitkorkul A., van de Lindt, J.W. (2010). Seismic response of a full-scale light-frame wood building: Experimental study. J. Struct. Eng., 136 (3), 246–254.

[14] Benavent-Climent A., Pujades Ll.G., López Almansa F. (2002). Design energy input spectra for moderate seismicity regions. Earthquake Engineering & Structural Dynamics. 31 1151-1172.

[15] Benavent-Climent A., López-Almansa F., Bravo-González D.A. (2010). Design energy input spectra for moderate-to-high seismicity regions based on Colombian earthquakes. Soil Dynamics & Earthquake Engineering. Vol. 30, No. 11, 1129-1148.

[16] López-Almansa F., Yazgan U., Benavent-Climent A. (2013). Design energy input spectra for high seismicity regions based on Turkish registers. Bulletin of Earthquake Engineering. Vol. 11, No. 4 885–912. DOI 10.1007/s10518-012-9415-2.

[17] Yazgan U. (2012). Proposal of energy spectra for earthquake resistant design based on Turkish registers. Doctoral Dissertation. Technical University of Catalonia.

[18] ANSI/AF&PA SDPWS (2008). ASD/LRFD Wind & Seismic. Special Design Provisions for Wind and Seismic. American Forest & Paper Association. American Wood Council.

[19] Thurston S.J., Park S.G. (2004). Seismic Design of New Zealand Houses. Bulletin of the New Zealand Society for Earthquake Engineering. Vol. 37, No. 1, 1-12.

[20] Housner G.W. (1956). Limit design of structures to resist earthquakes, Proceedings of First World Conference on Earthquake Engineering 5 1-12.

[21] Soong T.T., Dargush G. (1997). Passive energy Dissipation Systems in Structural Engineering. John Wiley.

[22] Foti D., Bozzo L.M., López Almansa F. (1998). Numerical Efficiency Assessment of Energy Dissipators for Seismic Protection of Buildings. Earthquake Engineering & Structural Dynamics. 27 543-556.

[23] Dinehart D.W., Shenton H.W., Elliott T.E. (1999). The dynamic response of wood-frame shear walls with viscoelastic dampers, Earthquake Spectra 15 (1), 67–86.

[24] Filiatrault A. (1990). Analytical predictions of the seismic response of friction damped timber shear walls, Earthquake Eng. Struct. Dyn. 19, 259–273.

[25] Higgins C. (2001). Hysteretic dampers for wood frame shear walls. Proc. of the 2001 Structures Congress and

Exposition, ASCE.
[26] Kawai N., Araki Y., Koshihara M., Isoda H. (2006). Seismic dampers for rehabilitating vulnerable Japanese wood houses. 9th World Conference on Timber Engineering (WCTE). Portland (USA).
[27] Matsuda K., Kasai K., Sakata H. (2012). Analytical Study on Passively Controlled 2-Story Wooden Frame by Detailed Frame Model. 15th World Conference on Earthquake Engineering (WCEE). Paper 3445. Lisbon.
[28] Palermo A., Sarti F., Baird A., Bonardi D., Dekker D., Chung S. (2012). From Theory to Practice: Design, Analysis and Construction of Dissipative Timber Rocking Post-Tensioning Wall System for Carterton Events Centre, New Zealand. 15th World Conference on Earthquake Engineering (WCEE). Paper 4617. Lisbon.
[29] Sarti F., Palermo A., Pampanin S. (2012). Simplified Design Procedures for Post-Tensioned Seismic Resistant Timber Walls. 15th World Conference on Earthquake Engineering (WCEE). Paper 36. Lisbon.
[30] Symans M.D., Constantinou M.C. (1998). Passive fluid viscous damping systems for seismic energy dissipation, Journal of Earthquake Technology, ISET, Special issue on passive control of structures, 35 (4), 185–206.
[31] Symans M.D., Cofer W.F., Friedley K.J. (2002). Base Isolation and Supplemental Damping Systems for Seismic Protection of Wood Structures: Literature Review. Earthquake Spectra Vol. 18, No. 3, 549-572.
[32] Soong T.T., Spencer B.F. (2002). Supplemental energy dissipation: state-of-the-art and state-of-the-practice. Engineering Structures 24 243–259.
[33] Palazzo G., López-Almansa F., Cahís X., Crisafulli F. (2009). A low-tech dissipative buckling restrained brace. Design, analysis, production and testing. Engineering Structures. Vol. 31, No. 9, 2152-2161.
[34] Akiyama H. (1985). Earthquake-resistant limit-state design for buildings, University of Tokyo Press, Tokyo.
[35] Fajfar P., Vidic T. (1994). Consistent inelastic design spectra: hysteretic and input energy, Earthquake Engineering and Structural Dynamics 23, 523-537.
[36] Priestley M.J.N., Calvi G.M., Kowalsky M.J. (2007). Displacement-Based Seismic Design of Structures, IUSS Press.
[37] Kuwamura H., Kirino Y., Akiyama H. (1994). Prediction of earthquake energy input from smoothed Fourier amplitude spectrum, Earthquake Engineering and Structural Dynamics 23, 1125-1137.
[38] Bertero R.D., Bertero V.V., Teran-Gilmore A. (1996). Performance-based earthquake-resistant design based on comprehensive design philosophy and energy concepts. Proceedings of the Eleventh World Conference on Earthquake Engineering, Disc 2, Paper No. 611.
[39] Chou C.C., Uang C.M. (2003). A procedure for evaluating seismic energy demand of framed structures. Earthquake Engineering and Structural Dynamics 32, 229-44.
[40] Jiao Y., Yamada S., Kishiki S., Shimada Y. (2011). Evaluation of plastic energy dissipation capacity of steel beams suffering ductile fracture under various loading histories. Earthquake Engineering and Structural Dynamics, 40 1553-1570 DOI: 10.1002/eqe.1103.
[41] Manfredi G. (2001). Evaluation of seismic energy demand. Earthquake Engineering & Structural Dynamics. 30:1 485-499.
[42] Decanini L.D., Mollaioli F. (2001). An energy-based methodology for the seismic assessment of seismic demand, Soil Dynamics and Earthquake Engineering 21, 113-137.
[43] FEMA 356. (2000). Prestandard and commentary for the seismic rehabilitation of buildings. Federal Emergency Management Agency.
[44] SEAOC. (1995). Vision 2000: Performance Based Seismic Engineering of Buildings, San Francisco.
[45] Benavent-Climent A. (2011). An energy-based method for seismic retrofit of existing frames using hysteretic dampers. Soil Dynamics & Earthquake Engineering. Vol. 31, 1385-1396.
[46] Milburn J., Banks W. (2004). Six-Level Timber Apartment Building in a High Seismic Zone. New Zealand Timber Design Journal 12 (3) 9-13.
[47] NZS 4203. (1992). New Zealand Code of practice for General Structural Design and Design Loadings for Buildings.
[48] NZS 1170.5 (2004). New Zealand Structural Design Actions. Part 5: Earthquake actions.
[49] Mahmoudi M., Zaree M. (2013). Performance based design using force reduction factor and displacement amplification factors for BFS. Asian journal of civil engineering. Vol. 14, No. 4 577-586.